Supporting Information

Article: *Constraining spectral models of a terrestrial gamma-ray flash from a terrestrial electron beam observation by the Atmosphere-Space Interactions Monitor*

Authors: *D. Sarria[1], N. Østgaard[1], P. Kochkin[1], N. Lehtinen[1], A. Mezentsev[1], M. Marisaldi[1], A. Lindanger[1], C. Maiorana[1], B. E. Carlson[1,2], T. Neubert[3], V. Reglero[4], K. Ullaland[1], S.Yang[1], G. Genov[1], B. H. Qureshi[1], C. Budtz-Jørgensen[3], I. Kuvvetli[3], F. Christiansen[3], O. Chanrion[3], J. Navarro-González[4], P. Connel[4], C. Eyles[4]*

1 : Birkeland Centre for Space Science, University of Bergen, Bergen, Norway

2 : Carthage College, Kenosha, Wisconsin, United States

3 : National Space Institute, Technical University of Denmark, Lyngby, Denmark

4 : University of Valencia, Valencia, Spain

This document aims to provide support to the main text about the weak dependence of the detected TEB spectrum on (1) the radial distance between the TEB center and the ISS, (2) the altitude of the source TGF (if set between 10 and 15 km), (3) the opening and the tilt angles of the source TGF. In section A, we present simulation results of the TEB energy spectra for the different set of parameters (radial distance, altitude, opening and tilt angles). Since the dependence on the TGF source altitude is the most noticeable (even if weak), we present in Section B the resulting tables of the full spectral analysis, but for TGF source altitudes of 10 and 15 km (the case of 12 km is considered in the main article). It demonstrate that the effect of the altitude is indeed weak . In section C, we present the binned energy spectra for LED and HED (and the combination) used to calculate the χ^2_r values in the main text.

A Parameter reduction for the energy spectrum analysis

In this section, we provide detailed justifications on why when performing spectral analysis on the Terrestrial Electron Beam (TEB), the shape of the recorded energy spectrum above 100 km altitude is only weakly

dependent on the following parameters:

- the radial distance between the TEB center and the ISS, see section A.1
- the altitude, if set between 10 and 15 km, see section A.2
- the opening and the tilt angles, see section A.3

This permits an essential parameter reduction to be able to perform a more constrained spectral analysis for the source TGF spectrum (producing the TEB), see the main text. However, these four parameters can have dramatic effect on the fluence (particles per cm^2) of the TEB, but this is not considered here because it only corresponds to a scale factor and has no effect on the spectral shape and the spectral analysis. Note also that this scale factor corresponds to the brightness of the source TGF and is a free parameter.

This key feature permits a big simplification of the problem as it reduces drastically the number of free parameters to include in the analysis. However, compared to TGF-only simulations, TGF+TEB simulations also present some disadvantages:

- they require more computation time, as accounting for electron/positron propagating in a large scale (Earth) magnetic field is much more computationally expensive than simulating only photon propagation.
- no detector response matrix can be used (this is only possible for incident photons) hence simulations using the full mass model must be performed for each source TGF spectrum, that is also computationally much more expensive.

In the following we present several simulated TEB energy spectra at satellite altitude (about 400 km for the ISS). They would be similar if detected anywhere between 100 km altitude and the satellite's altitude, because the remaining atmosphere above ≈100 km is very thin and cannot affect significantly the energetic electrons/positrons (> 400 keV). The presented spectra are also shown with a minimal energy of 400 keV, because electrons with lower energies are not expected to be detected by ASIM. Positrons with energies < 400 keV will produce pairs of 511 keV photons after annihilating after losing all their kinetic energy in the material surrounding the detectors. For all the simulations presented in this supporting information, the source TGF is assumed to have a standard fully-developed RREA spectrum $\propto 1/E \exp(-E/\epsilon)$, $\epsilon = 7.3$ MeV. Throughout the document, the energy spectrum curves are normalized to be equal to 1 at 1 MeV. Note that the choice of normalization does not really matter as it can be arbitrary, depending on the source brightness, that has a large range possible values ($\sim 10^{16}$ to $\sim 10^{20}$).

A.1 Effect of the radial distance between detector and TEB's center

For clarity, Figure A.1 presents a sketch to define the concept of radial distance. Figure A.2 shows simulations results of TEB electron energy spectra (at satellite altitude) inside several radial distance rings between the center of the TEB and the detector. The spectrum of a TEB only weakly varies with the radial distance between the TEB center and the detector. This is because electrons/positrons produced at a similar altitude, 80 km apart, have similar energy distribution. In addition the gyration motion of electrons/positrons along field lines also shuffles their positions. Above a radial distance of 80 km, we may observe a more significant difference (though we did not reach enough statistics in our simulations to check this precisely). In addition, 80 km from the center, the fluence (particles/cm^2) is about 25 times lower than in the center (point 0) and decreases even more with increasing radial distance, hence it is much less likely that the TEB could be detected from there.

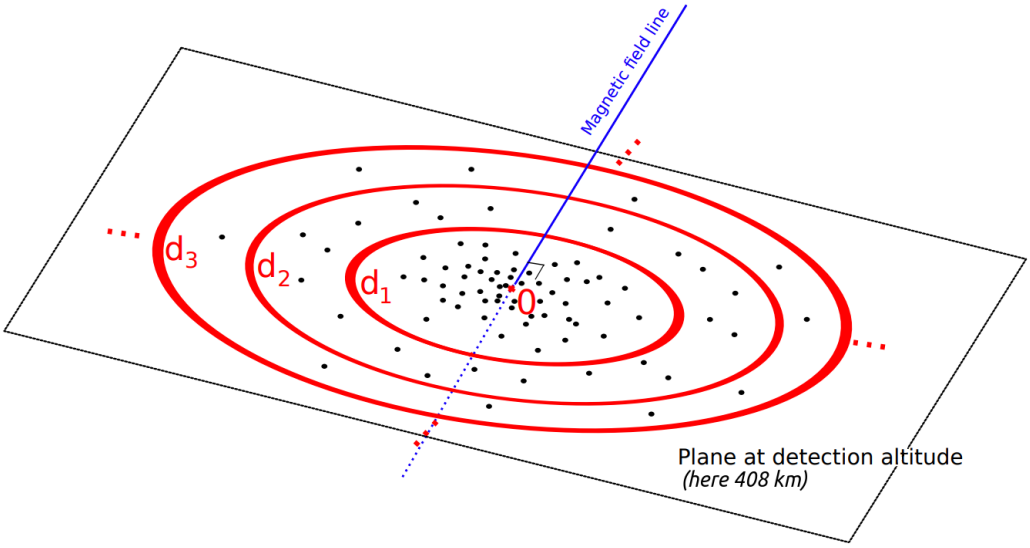

Figure A.1: Illustration of the concept of radial distance. The 0 is the center of the electron beam. The radial distance in the distance between this 0 and another point in the plane. The black dots represent the positions of electrons or positrons (there are millions of particles in the actual simulation data). The red rings are radial distance intervals at which electrons are collected. The spectra presented in Figure A.2 are built at given radial distance intervals.

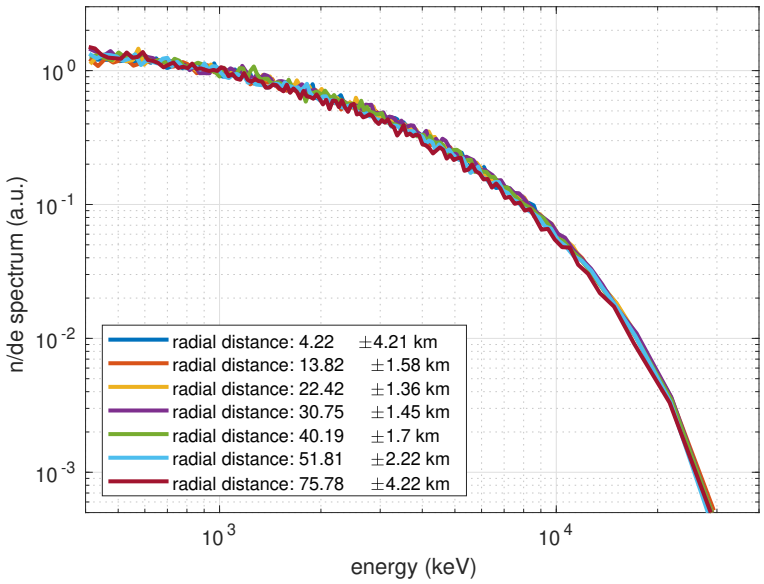

Figure A.2: TEB electron energy spectrum inside several radial distance rings between the center of the electron beam and the detector. The radial distance bins (i.e. intervals) and the energy bins are chosen to contain a similar number of particles. We observe very minor differences for any of the tested radial distances.

A.2 Effect of the altitude of the source TGF

The high energy part of the TGF spectrum (> 4 MeV) is affecting the production of energetic electrons and positrons (able to escape the atmosphere). This part of the spectrum remains similar after propagation to ≈ 100 km (and therefore higher altitudes since the effect of the atmosphere becomes negligible above) if the TGF source is placed from 10 km to 15 km altitude (in the main text, an altitude of 12 km is set). However, we may observe a more important variability for a broader altitude range but it is not relevant for TGFs. To justify qualitatively the previous statements, we performed extensive Monte-Carlo simulations. Figure A.3 presents the results, together with a quantification of the differences (lower panel). The resulting TEB spectra show a relative difference of less than 20% (absolute value) for most of the energy range, with an average of about 12% (absolute value). With only this information, we concede that it is not obvious that the source altitude will have only a weak effect on the results of the spectral analysis. This is why we also proceeded to the full spectral analysis for source TGF altitudes of 10 and 15 km, and built tables like Table 1 but for these source TGF altitudes. They are shown as Tables B.1 and B.2 (Table in the main text 1 is for 12 km). By looking at these tables, we can confirm that the TGF source altitude has only a weak effect on the results of the spectral analysis.

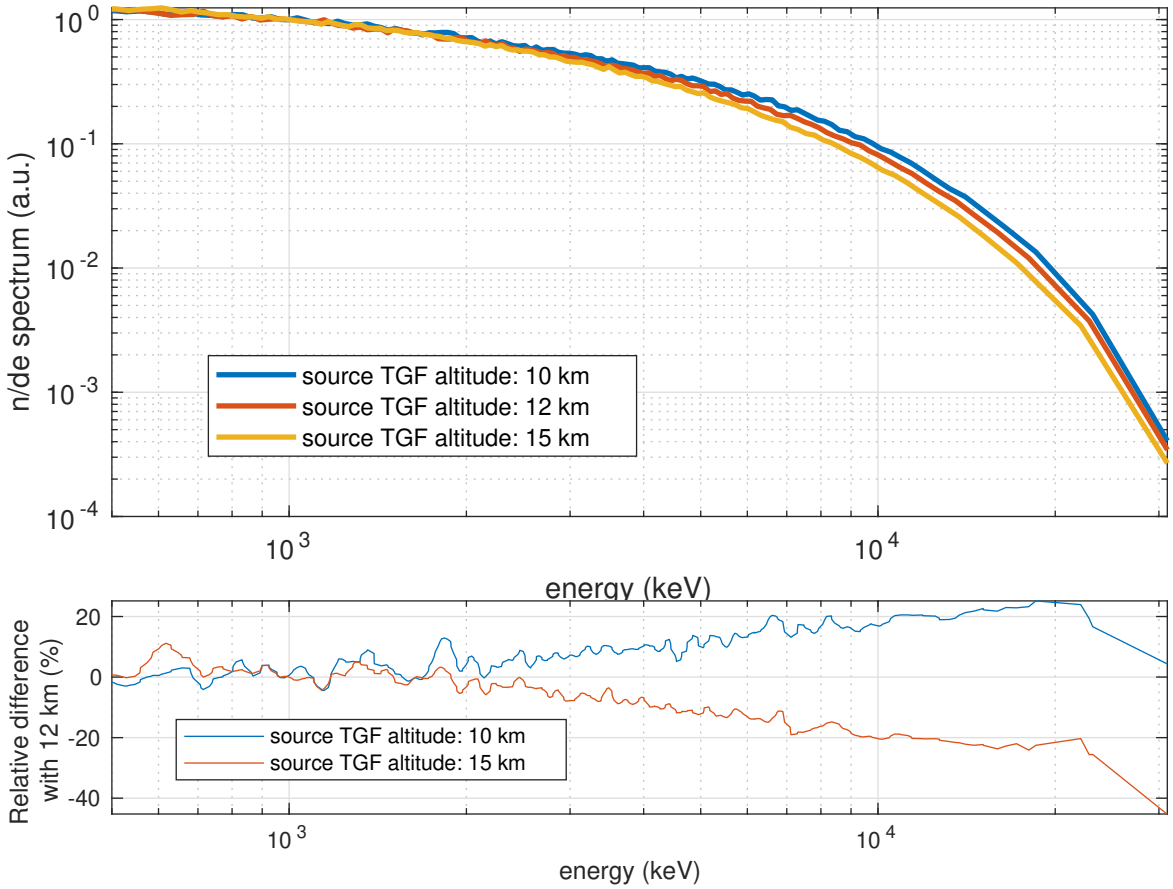

Figure A.3: Simulation results. The energy bins are chosen to contain a similar number of particles. TEB energy spectrum at satellite altitude, assuming different source TGF altitudes. Relatively small differences are observed.

A.3 Effect of the beaming and tilt angles of the source TGF

TGFs photons are forming a beam that is parameterized by an angle σ_θ (the source TGF is assumed to be beamed as a cone to make the discussion easier) and a tilt angle ρ with respect to the local vertical. We define the tilt angle ρ as follow: consider a plane defined by the TGF beam (center) direction, the local magnetic field direction and the TGF source (point) location. The tilt angle ρ as the angle the center of TGF beam is making with the local vertical (upwards), in the previous plane.

For this event, the angle between the direction of the local magnetic field and the local vertical is 58^o. Usual tilt angles associated to intra-cloud lightning leaders (attributed to TGF, at least the ones detected from space) are between ± 5 and ± 40 degrees with respect to the local vertical (*Lyu et al.*, 2016; *Mailyan et al.*,

2019). Figure A.4 is an illustration of qualitative arguments to justify why the TEB energy spectrum is not significantly affected by both the opening angle of the TGF and its tilt. The electrons/positrons that will be ultimately detected are only the ones that are produced between $\approx$ 40 and $\approx$ 100 km altitude (*Sarria et al.*, 2015), inside a geomagnetic field line "tube" that extends to the satellite. The energy spectrum of these electrons has no reason to change if the opening angle of the source TGF is increased or decreased. It has also no reason to change if the source TGF is slightly tilted (0^o to 5^o). If the source TGF is tilted towards the field line with larger angles, than the electron/position spectrum has no reason to change. If the beam is tilted largely away from the magnetic field "tube", then the TEB will not be detected by the satellite. For intermediate tilt angles (5^o to 40^o) we cannot provide qualitative arguments, but the effect was evaluated using simulations. We show in Figure A.5 and A.6 results of Monte-Carlo simulation assuming several opening angle values ($\sigma = 5^o, 12^o, 20^o, 30^o$) and tilt angles ($\rho = -40^o, -20^o, -10^o, -5^o, 0^o, 5^o, 10^o, 20^o, 40^o$). These simulations results confirm that the effect of varying σ_θ or ρ has indeed a very weak effect on the TEB energy spectrum.

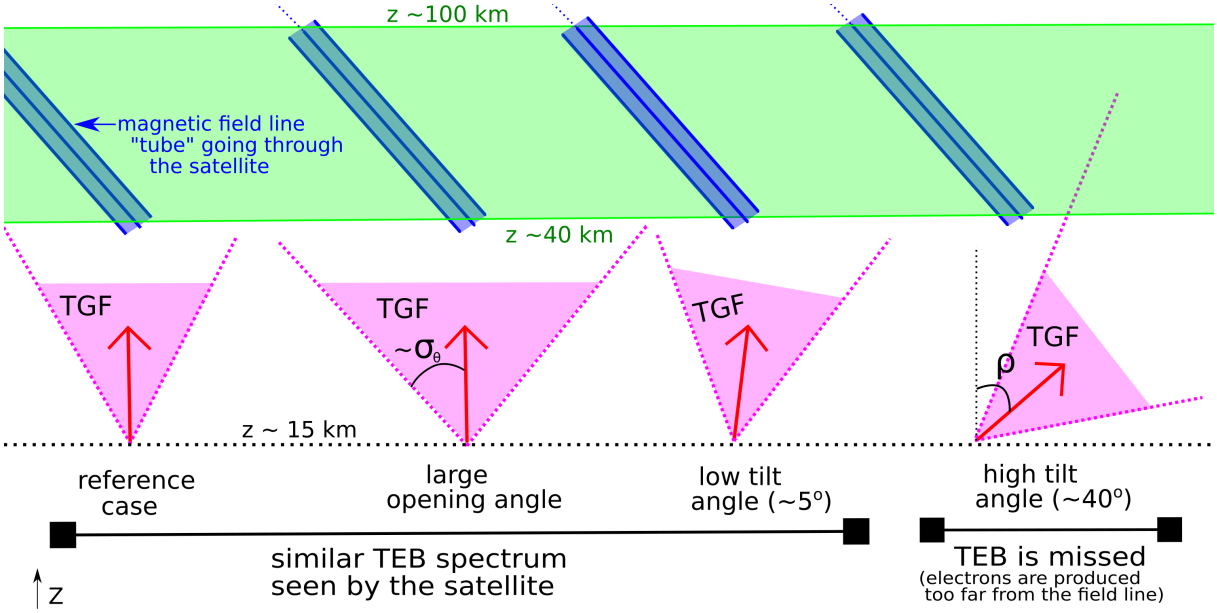

Figure A.4: Illustration of the effect of the angular distribution of the source TGF (a.k.a. beaming), i.e. when increasing the opening angle or tilting the photon beam. The source TGF is assumed to be beamed as a cone for simplicity. The electrons that are going to be eventually detected are produced between 40 and 100 km altitude along a specific geomagnetic field line tube. The energy spectrum of these electrons has no reason to change if the beaming is wider or tilted. If the tilt angle is too large, but in this case no (or very little) electrons are produced within the required area. The energy bins are chosen to contain a similar number of particles.

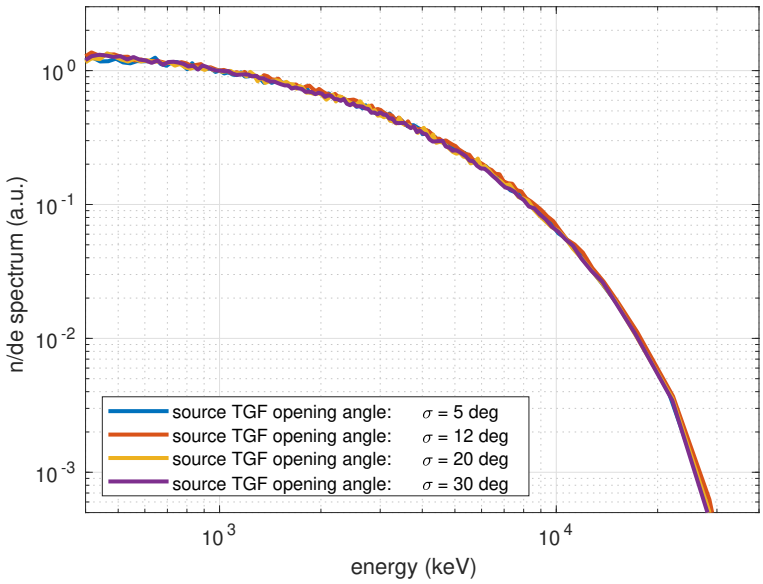

Figure A.5: Simulation results. The energy bins are chosen to contain a similar number of particles. TEB energy spectrum at satellite altitude, assuming different source TGF opening angles (σ_θ). All the tested values do not show significant difference.

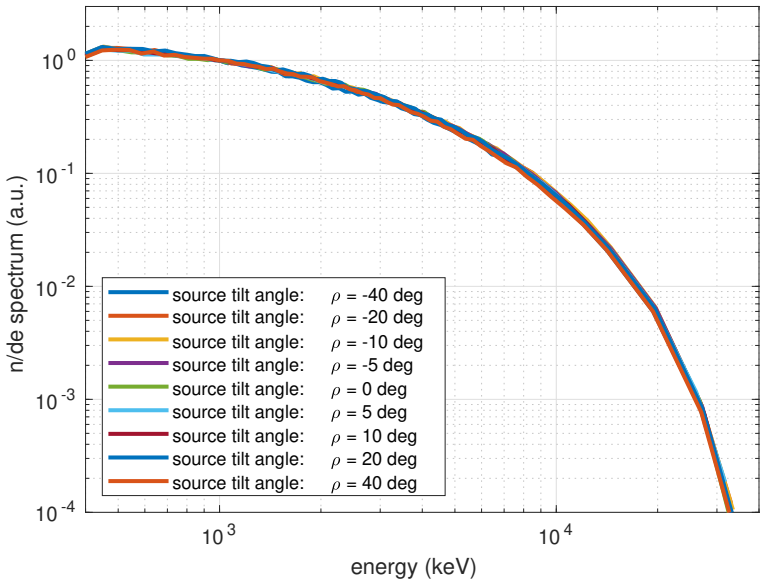

Figure A.6: Simulation results. The energy bins are chosen to contain a similar number of particles. TEB energy spectrum at satellite altitude, assuming different source TGF tilt angles (ρ) with respect to the local vertical. No significant difference is observed between the different parameters.

B Result Tables for a TGF source at 10 and 15 km altitude

In this section we present result tables of the the comparison of the tested spectral models with the measurement. In the main article, the table for a source TGF altitude of 12 km is presented, and here we present tables for a source at 10 and 15 km. We provide these tables because it is not obvious if the effect of the source TGF altitude on the TEB spectrum is weak or not, just based the TEB energy spectrum (Figure A.3). We can see that for both tables B.1 and B.2, the conclusions are the same as for the table for the 12 km case (that is Table 1 in the main article). This result confirms that the effect of the TGF source altitude is weak between 10 and 15 km and does not affect our conclusions in the main article.

Model	Effective area in cm^2		Effective area ratio	Maximum likelihood analysis result Δ_{mle}			Pearson's χ^2_r			e^+/e^- ratio
	LED	HED		LED	HED	Co.	LED	HED	Co.	
"Leader 160 MV" $\varepsilon = 4.3$ MeV $E_m = 19.2$ MeV	122.7	46.8	2.62	**0**	17.51	21.65	**0.87**	1.77	1.61	11.1%
"Leader 300 MV" $\varepsilon = 4.7$ MeV $E_m = 32$ MeV	147.5	67.6	2.18	**0**	**2.20**	6.78	**0.90**	**0.97**	**1.29**	14.6%
$\varepsilon = 6.5$ MeV $E_m = 40$ MeV	160.8	81.0	**1.98**	**0.06**	**0.18**	**2.98**	**0.90**	**0.81**	**1.26**	15.9%
$\varepsilon = 7.3$ MeV $E_m = 40$ MeV	163.5	86.0	**1.90**	**0.56**	**0**	**1.79**	**0.91**	**0.80**	**1.27**	16.9%
$\varepsilon = 8$ MeV $E_m = 40$ MeV	167.3	89.9	**1.86**	**0.17**	**0.21**	**0.99**	**0.90**	**0.81**	**1.27**	17.4%
$\varepsilon = 10$ MeV $E_m = 40$ MeV	177.7	100.3	**1.77**	**0**	**2.66**	**0**	**0.94**	**0.81**	**1.31**	19.3%
Compatibility range	n.a.		1.82±0.35	≤ 5			≤ 1.94	≤ 1.75	≤ 1.57	n.a.

Table B.1: ***For a TGF source altitude of 10 km.*** *Table summarizing the comparison of the tested spectral models with the measurement. Three main criteria are presented: the LED/HED effective area ratio, the maximum likelihood and the Pearson's χ^2_r. "Co." stands for the LED and HED combination. The compatibility range for the different criteria are also indicated. Bold values indicate compatible models for the given criterion.*

Model	Effective area in cm^2		Effective area ratio	Maximum likelihood analysis result Δ_{mle}			Pearson's χ^2_r			e^+/e^- ratio
	LED	HED		LED	HED	Co.	LED	HED	Co.	
"Leader 160 MV" $\varepsilon = 4.3$ MeV $E_m = 19.2$ MeV	127.7	43.8	2.92	**0.06**	20.28	23.00	0.86	**1.91**	1.63	9.3%
"Leader 300 MV" $\varepsilon = 4.7$ MeV $E_m = 32$ MeV	149.12	61.8	2.41	**0.34**	**4.33**	7.50	**0.86**	**1.00**	**1.27**	12.0%
$\varepsilon = 6.5$ MeV $E_m = 40$ MeV	157.4	73.5	**2.14**	**0.18**	**1.29**	**3.29**	**0.88**	**0.90**	**1.26**	13.9%
$\varepsilon = 7.3$ MeV $E_m = 40$ MeV	165.8	78.4	**2.11**	**0.37**	**0.51**	**1.97**	**0.89**	**0.83**	**1.25**	14.6%
$\varepsilon = 8$ MeV $E_m = 40$ MeV	169.9	83.6	**2.03**	**0.05**	**0.12**	**1.09**	**0.90**	**0.84**	**1.28**	15.7%
$\varepsilon = 10$ MeV $E_m = 40$ MeV	187.7	98.6	**1.90**	**0**	**0.50**	**0**	**0.91**	**0.81**	**1.29**	17.3%
Compatibility range	n.a.		1.82±0.35	≤ 5			≤ 1.94	≤ 1.75	≤ 1.57	n.a.

Table B.2: ***For a TGF source altitude of 15 km.*** *Table summarizing the comparison of the tested spectral models with the measurement. Three main criteria are presented: the LED/HED effective area ratio, the maximum likelihood and the Pearson's χ^2_r. "Co." stands for the LED and HED combination. The compatibility range for the different criteria are also indicated. Bold values indicate compatible models for the given criterion.*

C Spectrum comparison plot

In this section, we present the plot the spectra of the different models used to calculate the χ^2_r values in Table 1 of the main article. The source TGF is at an altitude of 12 km, has a Gaussian angular distribution with $\sigma = 20^o$ and no tilt angle (like in the main article). The showed energy binning for LED and HED is the same as the one used to calculate the χ^2_r. The results of the χ^2_r analysis are discussed in the main text.

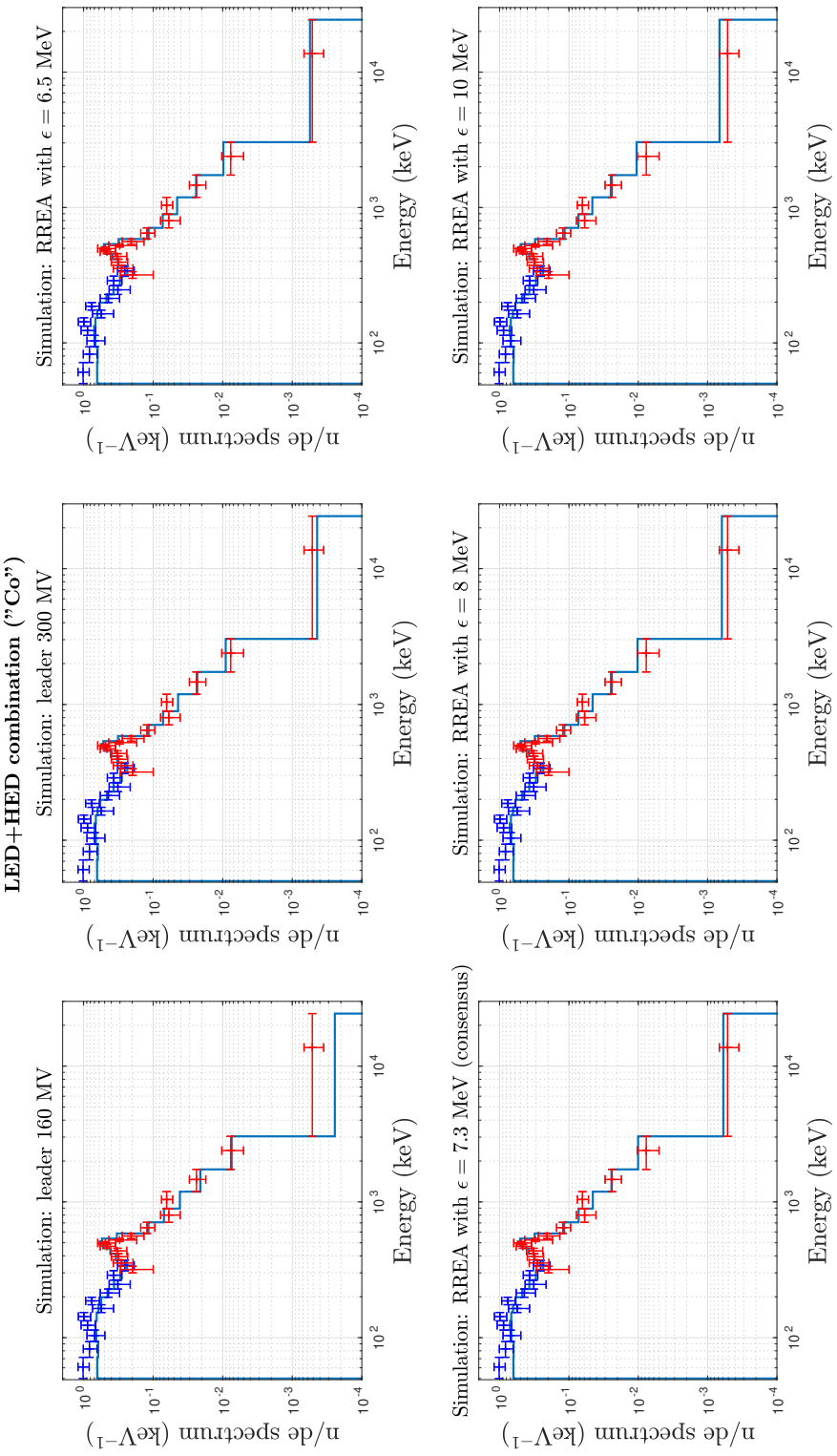

Figure C.1: Spectrum comparison between the TEB measurement, with both LED and HED, and the models described in the main article. The red and blue error bars are the measurement (identical for all subplots), and the blue histograms are the models.

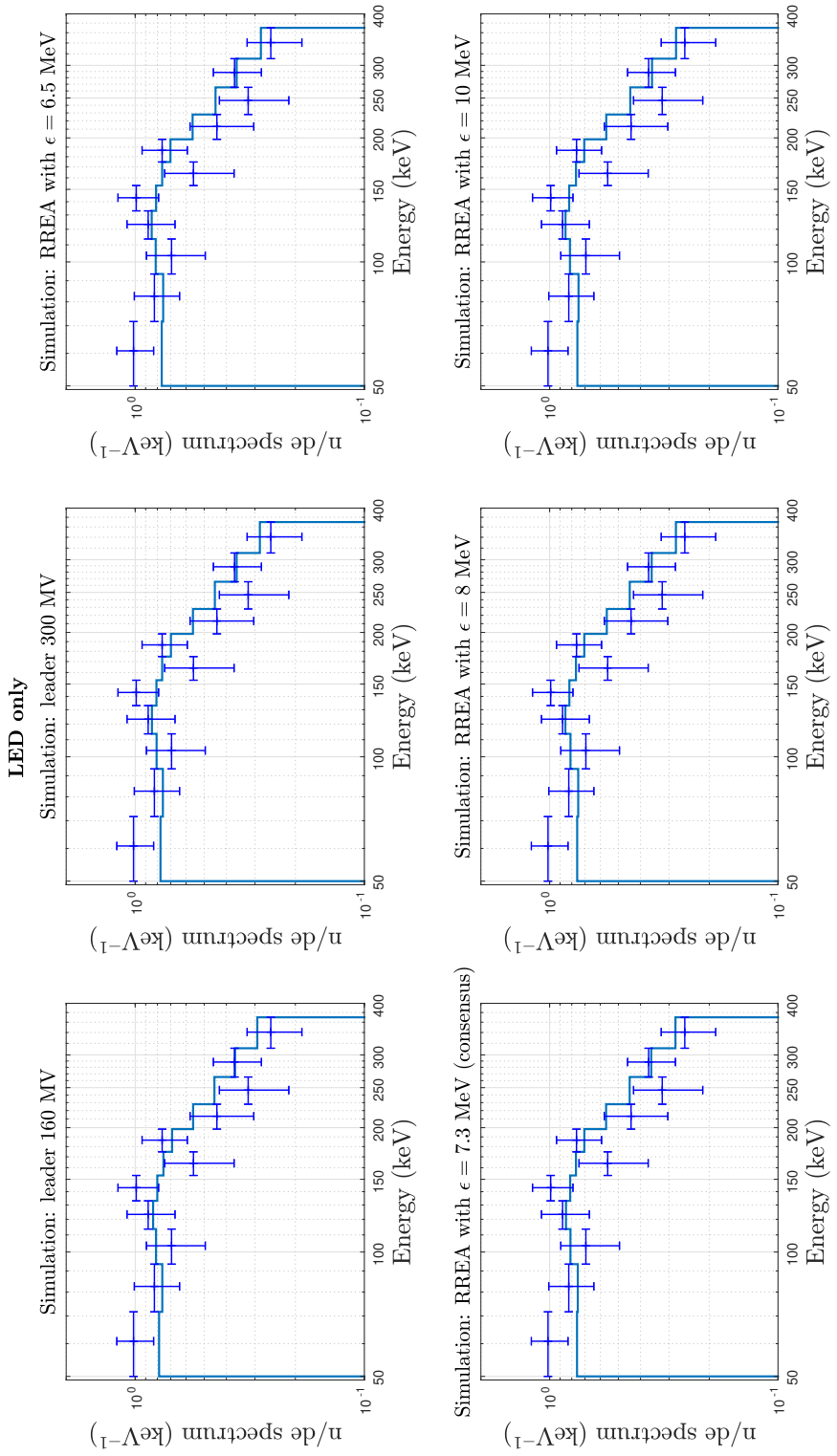

Figure C.2: Spectrum comparison between the TEB measurement, with only LED, and the models described in the main article. The blue histogram with error bars is the measurement (identical for all subplots), and the blue histograms are the models.

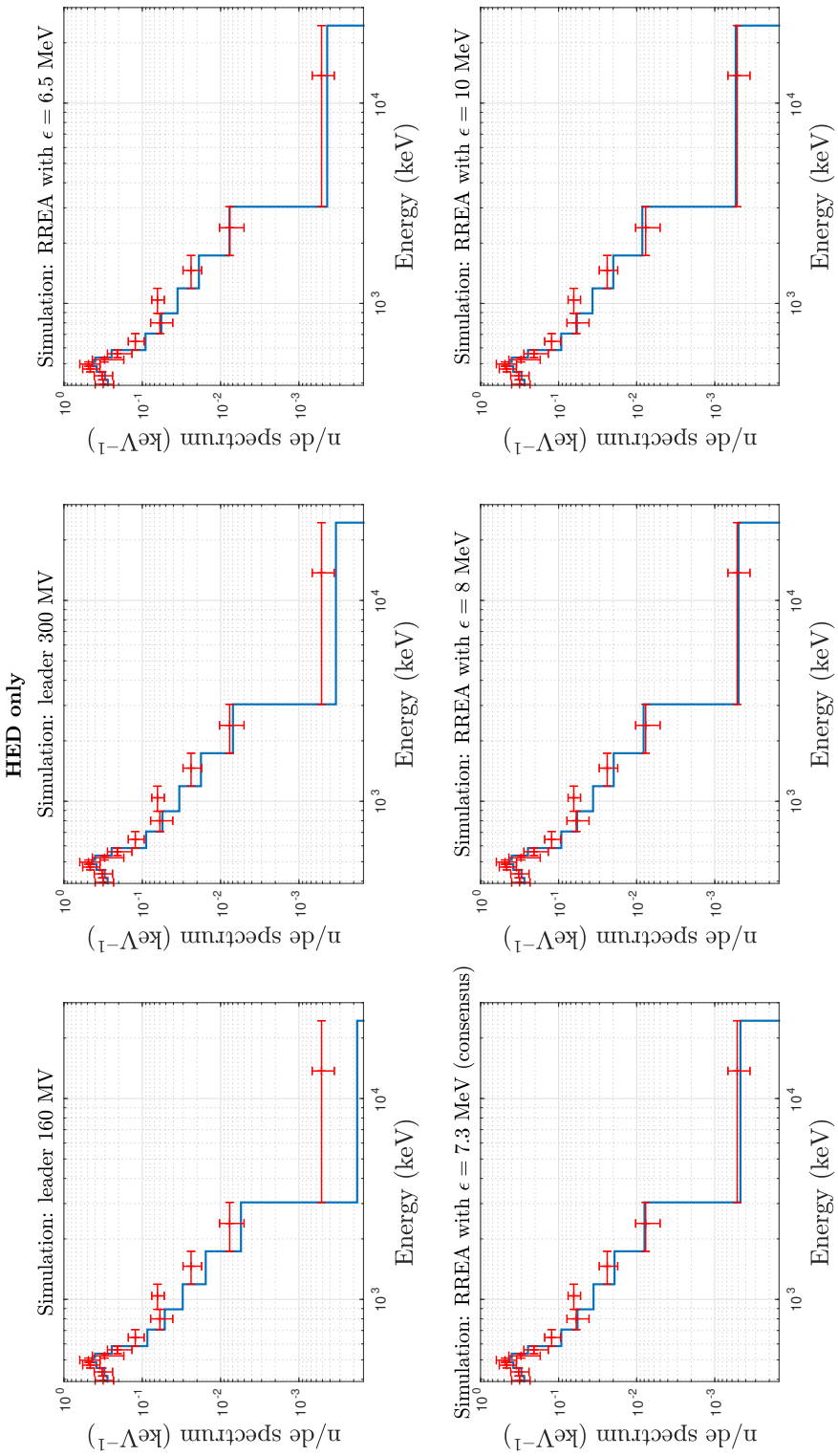

Figure C.3: Spectrum comparison between the TEB measurement, with only HED, and the models described in the main article. The red histogram with error bars is the measurement (identical for all subplots), and the blue histograms are the models.

References

Lyu, F., S. A. Cummer, G. Lu, X. Zhou, and J. Weinert, Imaging lightning intracloud initial stepped leaders by low-frequency interferometric lightning mapping array, *Geophysical Research Letters*, *43*(10), 5516–5523, doi:10.1002/2016GL069267, 2016.

Mailyan, B. G., W. Xu, S. Celestin, M. S. Briggs, J. R. Dwyer, E. S. Cramer, O. J. Roberts, and M. Stanbro, Analysis of Individual Terrestrial Gamma-Ray Flashes With Lightning Leader Models and Fermi Gamma-Ray Burst Monitor Data, *Journal of Geophysical Research (Space Physics)*, *124*(8), 7170–7183, doi:10.1029/2019JA026912, 2019.

Sarria, D., P.-L. Blelly, and F. Forme, MC-PEPTITA: A Monte Carlo model for Photon, Electron and Positron Tracking In Terrestrial Atmosphere—Application for a terrestrial gamma ray flash, *Journal of Geophysical Research (Space Physics)*, *120*(5), 3970–3986, doi:10.1002/2014JA020695, 2015.